CORA Cork Open Research Archive
Cartlann Taighde Oscailte Chorcaí

Title	Ligand design for long-range magnetic order in metal-organic frameworks
Authors	Tiana, Davide;Hendon, Christopher H.;Walsh, Aron
Publication date	2014-09-23
Original Citation	Tiana, D., Hendon, C. H. and Walsh, A. (2014) 'Ligand design for long-range magnetic order in metal-organic frameworks', Chemical Communications, 50(90), pp. 13990-13993. doi: 10.1039/c4cc06433j
Type of publication	Article (peer-reviewed)
Link to publisher's version	http://pubs.rsc.org/en/content/articlepdf/2014/cc/c4cc06433j - 10.1039/c4cc06433j
Rights	© The Royal Society of Chemistry 2014. This article is licensed under a Creative Commons Attribution 3.0 Unported Licence - https://creativecommons.org/licenses/by/3.0/
Download date	2026-11-15 16:14:54
Item downloaded from	https://hdl.handle.net/10468/6419

UCC
University College Cork, Ireland
Coláiste na hOllscoile Corcaigh

ChemComm

COMMUNICATION

View Article Online
View Journal | View Issue

Open Access Article. Published on 23 September 2014. Downloaded on 7/3/2018 12:18:52 PM.
This article is licensed under a Creative Commons Attribution 3.0 Unported Licence.

Cite this: *Chem. Commun.*, 2014, **50**, 13990

Received 15th August 2014,
Accepted 23rd September 2014

DOI: 10.1039/c4cc06433j

www.rsc.org/chemcomm

Ligand design for long-range magnetic order in metal–organic frameworks†

Davide Tiana, Christopher H. Hendon and Aron Walsh*

We report a class of ligands that are candidates to construct metal–organic frameworks with long-range magnetic order between transition metal centres. Direct quantum chemical calculations predict Néel temperatures exceeding 100 K for the case of Mn.

Metal–organic frameworks (MOFs) represent a diverse collection of materials featuring both inorganic and organic motifs, arranging in highly-ordered, and often porous arrays. Their chemical diversity and porosity has been subject to research efforts in catalysis,[1–4] gas storage, separation and sensing,[5–7] and recently in electrically conducting devices.[8–11] Beyond these popular applications, MOFs also display interesting solid-state behaviour such as disorder,[12] ion conduction,[13] and magnetism.[14,15]

Magnetism in MOFs is particularly interesting as ordered arrays of magnetically active species pose opportunity for data storage, spin-frustrated catalysis and magnetosensing.[16] Reports of magnetic MOFs are becoming more frequent;[17–21] notable examples are that of HKUST-1 (featuring an antiferromagnetically coupled bis-Cu(II) paddlewheels, shown in Fig. 1b)[22] and many Mn(II) based MOFs.[23,24] There are also an increasing number of reports on tailor-made MOFs specifically designed to achieve ferroelectric, magnetic and multiferroic behaviour.[25–27]

The development of ligands to exploit magnetism in hybrid materials is an active area.[28,29] For example, magnetic frameworks have been obtained using N-donor heterocycles[30] with polycarboxylates.[31,32] Despite this progress, critical temperatures have been very low to date. While the understanding of magnetism in inorganic materials is well developed, for hybrid materials there are no design principles for obtaining high Curie (T_C) or Néel (T_N) temperatures.[33]

In general, magnetism in materials can be described by the coupling of individual magnetic moments through an exchange interaction (J). A simple example is shown in Fig. 1a (and Fig. 2),

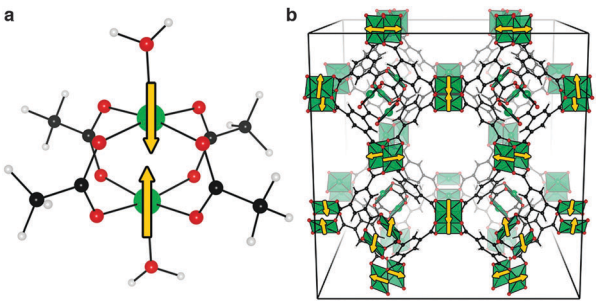


Fig. 1 The Cu–Cu paddlewheel exhibits an antiferromagnetic (open-shell singlet) magnetic ground-state in both the single molecule cupric acetate dihydrate, a, and the periodic metal–organic framework, HKUST-1, b. Schematic spin alignments are shown with arrows.

a dimer with two unpaired electrons can have two spin configurations, where $J = (E_S - E_T)/2$ is the energy difference between the singlet (S) and the triplet (T) states. If $J > 0$ the parallel spin configuration (ferromagnetic state, FM) is favoured. Conversely, the anti-parallel (antiferromagnetic state, AFM) spin configuration is favoured if $J < 0$. For example, cupric acetate dihydrate (Fig. 1a), a molecular analogue of the HKUST-1 hybrid framework, is an organometallic molecule with a range of accessible spin configurations.[34,35]

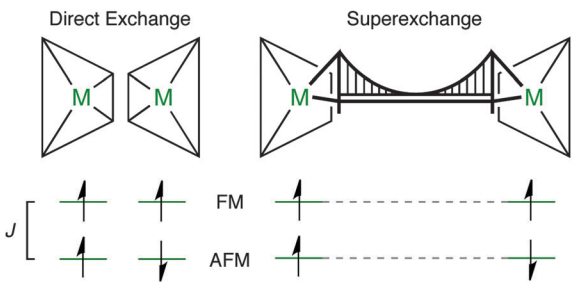


Fig. 2 The exchange energy, J, is determined by the energy difference between the singlet and the triplet states for a spin 1/2 dimer. Direct exchange is observed in spin-polarised metals in close proximity (*e.g.* the paddlewheel motif found in some metal–organic frameworks). Super-exchange is mediated by a diamagnetic bridging motif (*e.g.* the oxide ion in Mn–O–Mn).

Department of Chemistry, University of Bath, Claverton Down, Bath, BA2 7AY, UK. E-mail: a.walsh@bath.ac.uk

† Electronic supplementary information (ESI) available. See DOI: 10.1039/c4cc06433j

This journal is © The Royal Society of Chemistry 2014

Open Access Article. Published on 23 September 2014. Downloaded on 7/3/2018 12:18:52 PM.
This article is licensed under a Creative Commons Attribution 3.0 Unported Licence.

Direct magnetic exchange only occurs when there is electronic wavefunction overlap between the two magnetic sites. In most MOFs, the metal–metal distance will be too large for this to occur. In contrast, super-exchange can be active over longer distances.[36] Usually, metal cations are coupled through a diamagnetic anion (which we have schematically represented as a bridging motif, Fig. 2). A typical example is MnO which displays AFM order with T_N = 118 K.[37] Each Mn(II) centre has a formal electronic configuration of $3d^5$ and the Mn–O–Mn angle is 180° in the rocksalt structure, which are both optimal for super-exchange following the Goodenough–Kanamouri rules.[38,39] Another criterion is orbital symmetry: here, the Mn e_g ligand field combination effectively overlaps with the oxide 2p orbitals. The aim of this study is to identify an organic ligand suitable for mediating long-range super-exchange in metal–organic frameworks.

In the solid state, the exchange energy must be generalised to include factors such as the spin quantum number (S), the coordination number (z) and the site occupation (N):

$$J = \frac{E_{AFM} - E_{FM}}{2NS^2z}$$

This exchange energy can then be used in the standard Heisenberg Hamiltonian, from which the critical temperature is recovered within the mean field approximation (Van Vleck's formula):[40]

$$T_C = \frac{2}{3}\frac{Jz}{k_B}S(S+1)$$

where T_C is the magnetic critical temperature and k_B is the Boltzmann constant. The underlying exchange interactions can also be qualitatively described in terms of molecular orbitals.[41–43]

In the HKUST-1 framework, a strong direct exchange interaction within a Cu(II)–Cu(II) motif is present, but the cupric pairs are too far apart (>8 Å) to display any long-range magnetic order. Indeed, super-exchange with carboxylates tends to occur only within the same COO head.[15] For the direct interactions between the two $3d^9$ centres, an exchange constant $J = -10$ meV is calculated with an associated critical temperature of 348 K. This critical temperature is consistent with the molecular analogue copper acetate, where $T_N \sim 280$ K.

For effective super-exchange, as discussed earlier, the valence shell of the transition metal (TM) should be half-filled (*e.g.* the Mn(II) or Fe(III) ions), and the TM–ligand–TM angle should be close to 180°.[38,39] Mn(II) is therefore an ideal metal, which readily forms metal–organic frameworks and can adopt tetrahedral or octahedral coordination environments. In MnO, the 2p atomic orbitals of a single oxide ion facilitate super-exchange, while in a metal–organic framework, the coupling must be along the molecular orbitals of the entire ligand.

An ideal ligand would have an extended π system and feature orthogonal terminal groups. The ligands most commonly used in MOFs are either planar or have frontier orbitals localised on a central aromatic ring. However, such characteristics are embodied in oligoynes terminated in carboxylate groups, which are conjugated molecules with a helical continuous π wavefunction.[44] Their structural linearity may also allow so-called electron 'hopping' between metal centres. To our knowledge, there is only one example of a MOF featuring this ligand; however, it was constructed with the diamagnetic Zn(II) ion.[45]

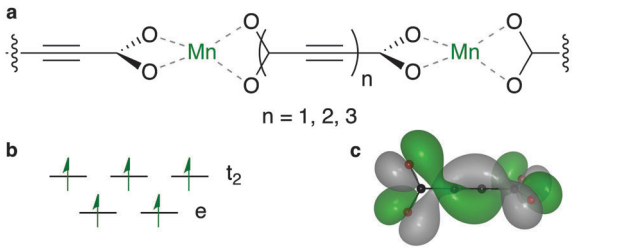


Fig. 3 Schematic representation of the Mn–ACDC–Mn conformation, a, that satisfies the basic requirements for long-range super-exchange. The smallest system (d(M–M) = 8.8 Å) is composed of high-spin Mn(II) ions in a tetrahedral ligand field, b, and one of the degenerate highest occupied molecular orbitals of the helically conjugated ACDC-1, c (isovalue 1×10^{-2} e A^{-3}). The combination of the two motifs to form a 1D framework results in a predicted Néel temperature of 117 K comparable to that of MnO.

Based on the considerations presented above, we have constructed a series of model systems combining Mn(II) and oligoyne dicarboxylates (Fig. 3). These one-dimensional coordination polymers are used as a model of the typical connectivity found in MOFs. In the smallest system, the Mn centres are linked by acetylene dicarboxylate (ACDC-1), which features orthogonal carboxylate motifs, and a single alkyne. The system is expanded by increasing the concatenation of the alkyne (*i.e.* the di-yne and tri-yne are reported as ACDC-2 and ACDC-3, respectively).

Analysis of the electronic structure reveals that five highest occupied crystal orbitals, are produced by the tetrahedral crystal field splitting of the Mn d shell. This TM orbital overlap with the O p_z produces a bonding interaction (see the ESI† for plots of all frontier orbitals). The lowest unoccupied crystal orbital is ligand centred, featuring the helical topology determined by single molecule calculations of the free ligand.[44] The higher energy unoccupied states are centred on the Mn–O interaction.

Due to the coordination environment, only orbitals with t_2 symmetry can yield electron hopping from one metal center to the other *via* O p orbitals (*i.e.* providing super-exchange interactions). Moreover, it has been recently emphasised how the correct directionality is also required for crystalline orbital to be fully delocalized through a coordination polymer.[46] Only the Mn d_{xz} and d_{yz} orbitals are active in our model system. These orbitals can combine with the helical highest molecular orbital of ACDC (Fig. 3c). The associated spin density (Fig. 4) illustrates the strong polarisation of the terminal carboxylate groups of the ligand. The changes in magnetic structure are described in Table 1; the electronic structure changes are further explored in the ESI.†

As a result of the half-filled d shell of Mn, and the Pauli exclusion principle, the FM configuration is disfavoured. In the most extreme case, MnACDC-1 (Fig. 4), $\Delta E = -22$ meV, with the AFM state being favoured (*i.e.* $\Delta E = E_{AFM} - E_{FM}$). The strength of the interaction is remarkable given the large metal–metal separation. The associated exchange constant is −0.86 meV, which corresponds to a mean field T_N of 117 K (Table 1) for this model system. This value is remarkably similar to the inorganic solid MnO, where the Mn–Mn separation is close to 3 Å.

Open Access Article. Published on 23 September 2014. Downloaded on 7/3/2018 12:18:52 PM.
This article is licensed under a Creative Commons Attribution 3.0 Unported Licence.

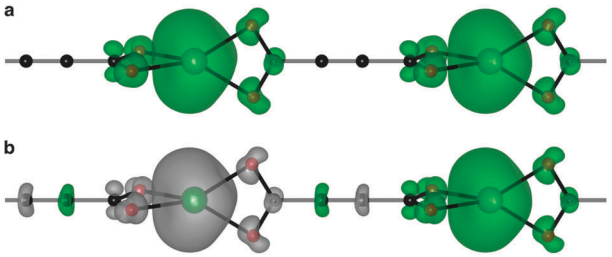


Fig. 4 The ferromagnetic (a) and antiferromagnetic (b) spin densities ($\rho^{\uparrow} - \rho^{\downarrow}$) of MnACDC-1 (isovalue 3×10^{-2} e Å^{-3}). The ground-state magnetic configuration is AFM; note the strong polarisation of the terminal carboxylate groups and the spin contributions from the diamagnetic ligand for the AFM case.

Table 1 Structural and magnetic parameters of MnACDC-*n* at the DFT-PBEsol level of theory. The metal–metal distance (d(M–M)) is listed in Å, the difference between AFM and FM states (ΔE) and the exchange energy (J) are in meV, and the Néel temperature (T_N) in K

n	d(M–M)	ΔE	J	T_N
1	8.8	−22	−0.86	117
2	11.4	−10	−0.38	51
3	14.0	−5	−0.20	26

The behaviour predicted for MnACDC-1 holds true for longer oligoynes, with J decreasing proportional to d(M–M). The exponential decay is characteristic of a super-exchange interaction[47] (see ESI†). Examining MnACDC-2, d(M–M) increases to 11.4 Å. Similar to the monoalkyne, the same local magnetic moment is calculated for Mn(II) and the AFM state is the most stable; ΔE = −10 meV and T_N = 51 K. From the electronic point of view, the main difference between ACDC-1 and 2 is that the occupied orbitals are destabilised due to the longer π system. There is an associated reordering of the crystalline orbitals, with the ligand states occupying the higher energy frontier orbitals (see ESI†). This change shields the two metals, reducing their magnetic coupling. The effect is further enhanced for ACDC-3 where d(M–M) increases to 14 Å. Here the energy difference reduces to 5 meV, corresponding to T_N = 27 K.

To demonstrate the generality of the approach, additional calculations were performed on an analogous (n = 1) Mn polymer with octahedral coordination (*via* two axial water molecules). Here the energy difference is 19 meV, corresponding to T_N = 105 K. Full details are given in the ESI.†

In summary, by considering the type of magnetic interactions that can take place in metal–organic frameworks, a series of simple rules for facilitating long-range magnetic order have been presented. We have shown that the paddlewheel motif, found in MOFs such as HKUST-1, can exhibit a strong direct exchange interaction that may later be harnessed for magneto-sensing. Further, the principles of super-exchange have been used to tailor hybrid materials with high critical temperatures, comparable to magnetic oxides, even though the separation between the spin polarised metals is in excess of 8 Å. It is evident that combining extended conjugated linear organic molecules with transitions metals is an effective approach to achieve long-range hybrid super-exchange. We hope that this work will stimulate experimental efforts to synthesise three-dimensional frameworks based on these components.

Computational details. All calculations were performed within the solid-state quantum chemical code Quantum Espresso (version 5.0.2)[48] at the density functional level of theory. The semi-local PBEsol exchange correlation functional was employed for ionic relaxation,[49] using norm-conserving pseudopotentials with a cut-off of 80 Ry. Dispersion force corrections were also employed.[50,51]

Nine k-points along the polymer axis were generated with the Monkhorst–Pack grid.[52] The force and energy thresholds were set to 5×10^{-3} eV and 5×10^{-4} eV, respectively, for geometry optimisation. The spin state of single atoms were allowed to relax during the optimisation with an SCF convergence threshold of 1×10^{-6} eV.

In order to test the dependence on the treatment of electron exchange and correlation, additional calculations were performed using the local LDA[53] and non-local hybrid HSE06 level of theory.[54] We also tested the inclusion of spin–orbit coupling, which made no notable difference to the results. A further comparison with PAW pseudopotential was also performed (see the ESI† for further details).

This study was inspired by A. K. Cheetham's lecture at MC11. C.H.H. thanks N. F. Chilton for useful discussions on magnetism. D.T. and C.H.H. are funded by the ERC (Grant No. 277757). A.W. acknowledges support from the Royal Society University Research Fellowship scheme. The work benefits from the high performance computing facility at the University of Bath. Access to the HECToR supercomputer was facilitated through membership of the HPC Materials Chemistry Consortium (EP/F067496). Images of chemical structures and orbitals were made using the VESTA software.[55] This work made use of the software package GNU Octave, and the authors are grateful for the support of the Octave development community.[56]

References

1 C. H. Hendon, D. Tiana, M. Fontecave, C. Sanchez, L. D'arras, C. Sassoye, L. Rozes, C. Mellot-Draznieks and A. Walsh, *J. Am. Chem. Soc.*, 2013, **135**, 10942.
2 J. Liu, L. Chen, H. Cui, J. Zhang, L. Zhang and C.-Y. Su, *Chem. Soc. Rev.*, 2014, **43**, 6011.
3 T. Zhang and W. Lin, *Chem. Soc. Rev.*, 2014, **43**, 5982.
4 K. T. Butler, C. H. Hendon and A. Walsh, *J. Am. Chem. Soc.*, 2014, **136**, 2703.
5 P. Falcaro, R. Ricco, C. M. Doherty, K. Liang, A. J. Hill and M. J. Styles, *Chem. Soc. Rev.*, 2014, **43**, 5513.
6 D. Britt, D. Tranchemontagne and O. M. Yaghi, *Proc. Natl. Acad. Sci. U. S. A.*, 2008, **105**, 11623.
7 J. B. Decoste and G. W. Peterson, *Chem. Rev.*, 2014, **114**, 5695.
8 M. D. Allendorf, A. Schwartzberg, V. Stavila and A. A. Talin, *Chem. – Eur. J.*, 2011, **17**, 11372.
9 C. H. Hendon, D. Tiana and A. Walsh, *Phys. Chem. Chem. Phys.*, 2012, **14**, 13120.
10 A. A. Talin, A. Centrone, A. C. Ford, M. E. Foster, V. Stavila, P. Haney, R. A. Kinney, V. Szalai, F. El Gabaly, H. P. Yoon, F. Léonard and M. D. Allendorf, *Science*, 2014, **343**, 66.
11 V. Stavila, A. A. Talin and M. D. Allendorf, *Chem. Soc. Rev.*, 2014, **43**, 5994.
12 T. D. Bennett and A. K. Cheetham, *Acc. Chem. Res.*, 2014, **47**, 1555.
13 P. Ramaswamy, N. E. Wong and G. K. H. Shimizu, *Chem. Soc. Rev.*, 2014, **43**, 5913.
14 D.-F. Weng, Z.-M. Wang and S. Gao, *Chem. Soc. Rev.*, 2011, **40**, 3157.
15 M. Kurmoo, *Chem. Soc. Rev.*, 2009, **38**, 1353.

 This journal is © The Royal Society of Chemistry 2014

Open Access Article. Published on 23 September 2014. Downloaded on 7/3/2018 12:18:52 PM.
This article is licensed under a Creative Commons Attribution 3.0 Unported Licence.

16 Given that electrically conducting MOFs are rare, there is an appeal to making a device based on change in magnetism rather than voltage.
17 L. M. Toma, C. Ruiz-Pérez, J. Pasán, W. Wernsdorfer, F. Lloret and M. Julve, *J. Am. Chem. Soc.*, 2012, **134**, 15265.
18 C. N. R. Rao, A. K. Cheetham and A. Thirumurugan, *J. Phys.: Condens. Matter*, 2008, **20**, 083202.
19 Z. Wang, P. Jain, K. Choi and J. V. Tol, *Phys. Rev. B: Condens. Matter Mater. Phys.*, 2013, 224406.
20 Y. Tian, W. Wang, Y. Chai, J. Cong, S. Shen, L. Yan, S. Wang, X. Han and Y. Sun, *Phys. Rev. Lett.*, 2014, **112**, 017202.
21 P. J. Saines, P. T. Barton, M. Jura, K. S. Knight and A. K. Cheetham, *Mater. Horiz.*, 2014, **1**, 332–337.
22 S. S. Chui, S. M. Lo, J. P. H. Charmant, A. G. Orpen and I. D. Williams, *Science*, 1999, **283**, 1148.
23 P. Jain, V. Ramachandran, R. J. Clark, H. D. Zhou, B. H. Toby, N. S. Dalal, H. W. Kroto and A. K. Cheetham, *J. Am. Chem. Soc.*, 2009, **131**, 13625.
24 A. F. Cozzolino, C. K. Brozek, R. D. Palmer, J. Yano, M. Li and M. Dincă, *J. Am. Chem. Soc.*, 2014, **136**, 3334.
25 W. Zhang and R.-G. Xiong, *Chem. Rev.*, 2012, **112**, 1163.
26 K.-L. Hu, M. Kurmoo, Z. Wang and S. Gao, *Chem. – Eur. J.*, 2009, **15**, 12050.
27 A. Stroppa, P. Jain, P. Barone, M. Marsman, J. M. Perez-Mato, A. K. Cheetham, H. W. Kroto and S. Picozzi, *Angew. Chem., Int. Ed.*, 2011, **50**, 5847.
28 X.-Y. Wang, Z.-M. Wang and S. Gao, *Chem. Commun.*, 2008, 281–294.
29 M. Pilkington, M. Gross, P. Franz, M. Biner, S. Decurtins, H. Stoeckli-Evans and A. Neels, *J. Solid State Chem.*, 2001, **159**, 262.
30 K. S. Murray, *Eur. J. Inorg. Chem.*, 2008, 3101.
31 M. Kurmoo, H. Kumagai, S. M. Hughes and C. J. Kepert, *Inorg. Chem.*, 2003, **42**, 6709–6722.
32 N. Guillou, C. Livage and G. Frey, *Eur. J. Inorg. Chem.*, 2006, 4963–4978.
33 A. K. Cheetham and C. N. R. Rao, *Science*, 2007, **318**, 58.
34 E. I. Solomon, B. L. Hemming and D. E. Root, *Electronic Structures of Active Sites in Copper Proteins: Coupled Binuclear and Trinuclear Cluster Sites*, Springer Netherlands, 1993, pp. 3–5.
35 P. K. Ross, M. D. Allendorf and E. I. Solomon, *J. Am. Chem. Soc.*, 1989, **111**, 4009.
36 J. Kanamori, *J. Phys. Chem. Solids*, 1959, **10**, 87.
37 P. W. Anderson, *Phys. Rev.*, 1950, **79**, 350.
38 J. B. Goodenough, *Magnetism and the Chemical Bond*, Wiley, Cambridge, MA, USA, 1963.
39 A. J. Tasiopoulos, A. Vinslava, W. Wernsdorfer, K. A. Abboud and G. Christou, *Angew. Chem., Int. Ed.*, 2004, **43**, 2117.
40 S. Blundell, *Magnetism in Condensed Matter*, Oxford University Press, Oxford, OX2 6DP UK, 2001.
41 P. J. Hay, J. C. Thibeault and R. Hoffmann, *J. Am. Chem. Soc.*, 1975, **97**, 4884.
42 H.-J. Koo, M.-H. Whangbo, P. D. VerNooy, C. C. Torardi and W. J. Marshall, *Inorg. Chem.*, 2002, **41**, 4664.
43 H.-J. Koo and M.-H. Whangbo, *Inorg. Chem.*, 2000, **39**, 3599.
44 C. H. Hendon, D. Tiana, A. T. Murray, D. R. Carbery and A. Walsh, *Chem. Sci.*, 2013, **4**, 4278.
45 D. Tranchemontagne, J. Hunt and O. Yaghi, *Tetrahedron*, 2008, **64**, 8553.
46 D. Tiana, C. H. Hendon, A. Walsh and T. P. Vaid, *Phys. Chem. Chem. Phys.*, 2014, DOI: 10.1039/C4CP00008K.
47 R. E. Coffman and G. R. Buettner, *J. Phys. Chem.*, 1979, **83**, 2387.
48 P. Giannozzi, S. Baroni, N. Bonini, M. Calandra, R. Car, C. Cavazzoni, D. Ceresoli, G. L. Chiarotti, M. Cococcioni, I. Dabo, A. Dal Corso, S. de Gironcoli, S. Fabris, G. Fratesi, R. Gebauer, U. Gerstmann, C. Gougoussis, A. Kokalj, M. Lazzeri, L. Martin-Samos, N. Marzari, F. Mauri, R. Mazzarello, S. Paolini, A. Pasquarello, L. Paulatto, C. Sbraccia, S. Scandolo, G. Sclauzero, A. P. Seitsonen, A. Smogunov, P. Umari and R. M. Wentzcovitch, *J. Phys.: Condens. Matter*, 2009, **21**, 395502.
49 J. P. Perdew, A. Ruzsinszky, G. I. Csonka, O. A. Vydrov, G. E. Scuseria, L. A. Constantin, X. Zhou and K. Burke, *Phys. Rev. Lett.*, 2008, **100**, 136406.
50 S. Grimme, *J. Comput. Chem.*, 2006, **27**, 1787.
51 V. Barone, M. Casarin, D. Forrer, M. Pavone, M. Sambi and A. Vittadini, *J. Comput. Chem.*, 2009, **30**, 934.
52 H. J. Monkhorst and J. D. Pack, *Phys. Rev. B: Solid State*, 1976, **13**, 5188.
53 J. P. Perdew and A. Zunger, *Phys. Rev. B: Condens. Matter Mater. Phys.*, 1981, **23**, 5048.
54 J. Heyd, G. E. Scuseria and M. Ernzerhof, *J. Chem. Phys.*, 2003, **118**, 8207.
55 K. Momma and F. Izumi, *J. Appl. Crystallogr.*, 2011, **44**, 1272.
56 J. W. Eaton, D. Bateman and S. Hauberg, *GNU Octave version 3.0.1 manual: a high-level interactive language for numerical computations*, CreateSpace Independent Publishing Platform, 2009.